HHS Public Access

Author manuscript

Proceedings (IEEE Int Conf Bioinformatics Biomed). Author manuscript; available in PMC 2024 January 02.

Published in final edited form as:

Proceedings (IEEE Int Conf Bioinformatics Biomed). 2022 December ; 2022: 1323–1328. doi:10.1109/bibm55620.2022.9995657.

Consistency of Graph Theoretical Measurements of Alzheimer's Disease Fiber Density Connectomes Across Multiple Parcellation Scales

Frederick Xu[†], **Sumita Garai**[‡], **Duy Duong-Tran**[‡], **Andrew J. Saykin**[§], **Yize Zhao**[¶], **Li Shen**[‡,*], **ADNI**[**]

[†]Department of Bioengineering, University of Pennsylvania, Philadelphia, USA

[‡]Department of Biostatistics, Epidemiology and Informatics, University of Pennsylvania, Philadelphia, USA

[§]Department of Radiology and Imaging Sciences, Indiana University, Indianapolis, USA

[¶]Department of Biostatistics, Yale University School of Public Health, NJ, USA

Abstract

Graph theoretical measures have frequently been used to study disrupted connectivity in Alzheimer's disease human brain connectomes. However, prior studies have noted that differences in graph creation methods are confounding factors that may alter the topological observations found in these measures. In this study, we conduct a novel investigation regarding the effect of parcellation scale on graph theoretical measures computed for fiber density networks derived from diffusion tensor imaging. We computed 4 network-wide graph theoretical measures of average clustering coefficient, transitivity, characteristic path length, and global efficiency, and we tested whether these measures are able to consistently identify group differences among healthy control (HC), mild cognitive impairment (MCI), and AD groups in the Alzheimer's Disease Neuroimaging Initiative (ADNI) cohort across 5 scales of the Lausanne parcellation. We found that the segregative measure of transtivity offered the greatest consistency across scales in distinguishing between healthy and diseased groups, while the other measures were impacted by the selection of scale to varying degrees. Global efficiency was the second most consistent measure that we tested, where the measure could distinguish between HC and MCI in all 5 scales and between HC and AD in 3 out of 5 scales. Characteristic path length was highly sensitive to the variation in scale, corroborating previous findings, and could not identify group differences in many of the scales. Average clustering coefficient was also greatly impacted by scale, as it consistently failed to identify group differences in the higher resolution parcellations. From these results, we conclude that many graph theoretical measures are sensitive to the selection of parcellation scale, and further development in methodology is needed to offer a more robust characterization of AD's relationship with disrupted connectivity.

[*]Correspondence to li.shen@pennmedicine.upenn.edu.

[**]Data used in preparation of this article were obtained from the Alzheimer's Disease Neuroimaging Initiative (ADNI) database (adni.loni.usc.edu). As such, the investigators within the ADNI contributed to the design and implementation of ADNI and/or provided data but did not participate in analysis or writing of this report. A complete listing of ADNI investigators can be found at: http://adni.loni.usc.edu/wp-content/uploads/how_to_apply/ADNI_Acknowledgement_List.pdf

Index Terms—

Network neuroscience; graph theory; structural connectome; multiscale parcellation; Alzheimer's disease

I. Introduction

Alzheimer's disease, the most common form of dementia characterized by an irreversible progressive memory loss followed by deterioration of cognitive function and memory recall, is currently afflicting over 6 million people in the United States with the number estimated to increase to 15 million by the year 2050 [1]. The disease's pathology has a complex relationship with anatomical deterioration and has long been considered as a disconnection syndrome where pathology may arise from disrupted efferent and afferent connections [2], leading it to receive much attention in network neuroscience where methods of quantifying complex connectivity disruptions are readily available [3]. Graph theoretical measurements that enable efficient characterization of brain network topology have been broadly applied to study Alzheimer's disease across many structural and functional imaging modalities, noting statistical differences in graph theoretical measurements among healthy control (HC), mild cognitive impairment (MCI), and AD subjects [4], [5].

However, there are inconsistencies across studies in the direction of change of the measurements and their discriminating power, resulting in a critical barrier of diverging interpretations of the relationship between disease state and network connectivity [6], [7]. The discrepancies may arise from differences in network construction methods, including but not limited to the selections of parcellation scheme, spatial resolution, and connection density [8]–[11]. These realizations have raised questions regarding how variations in the multitude of choices in network construction methods may influence the observed topological properties of diseased brain networks. Previous studies have noted sensitivity of characteristic path length, small-world index, and clustering coefficient to the number of nodes and density of brain networks [12]. In AD-specific research, it is noted that graph theoretical measures' capabilities of identifying population differences among AD diagnostic groups will vary based on parcellation scheme [13]–[16]. However, although different parcellation schemes offer varying resolutions and scales of a brain network, the comparisons between atlases are not strictly hierarchical as the regional boundaries in each parcellation scheme may not be identified in a consistent manner [17]. As such, a more controlled investigation across resolutions of the same parcellation scheme is needed.

To that end, our present study investigates the effect of parcellation scale, which governs the number of nodes in the brain network in a hierarchical manner, on the observed topological properties of AD-related white matter connectomes. We use fiber density networks derived from diffusion tensor imaging (DTI) tractography and observe the stability of graph theoretical measures across 5 scales of the Lausanne parcellation. To the best of our knowledge, fiber density has not been previously explored in this context. Our hypothesis is that graph theoretical measures will vary in observed significance between diagnostic

groups when the parcellation scale is changed, corroborating previous findings regarding the sensitivity of these measures to graph creation methods.

II. Materials and Methods

A. Data acquisition, preprocessing, and network construction.

Data used in the preparation of this article were obtained from the Alzheimer's Disease Neuroimaging Initiative (ADNI) database (adni.loni.usc.edu) [18], [19]. The ADNI was launched in 2003 as a public-private partnership, led by Principal Investigator Michael W. Weiner, MD. The primary goal of ADNI has been to test whether serial magnetic resonance imaging (MRI), positron emission tomography (PET), other biological markers, and clinical and neuropsychological assessment can be combined to measure the progression of mild cognitive impairment (MCI) and early AD. For up-to-date information, see www.adni-info.org.

DTI scans and demographic data were obtained from the Alzheimer's disease neuroimaging initiative (ADNI-GO/2) database [18]–[21]. The population consisted of 99 male and 74 female subjects. The population was age-controlled with the AD population averaging at 72.5 years, the MCI population averaging at 72.0 years, and the HC population averaging at 73.3 years. No significant difference in ages was detected across population groups (ANOVA: $P = 0.805$, $F = 0.217$). The DTI data were entered into an image processing pipeline, including denoising, motion-correction, and distortion-correction using an overcomplete local principal components analysis (PCA) [22]. Probabilistic white matter fiber tractography was then performed using a streamline tractography algorithm called fiber assignment by continuous tracking (FACT) [23].

Structural MRI (sMRI) scans were then registered to lower resolution b0 volume of the DTI data using the FLIRT toolbox in the FMRIB Software Library (FSL) [24] and cortical and subcortical brain regions of interest (ROIs) were defined based on the Lausanne parcellation [25]. The process was repeated for 5 scales of the Lausanne parcellation: 33, 60, 125, 250, and 500. The parcellation scales contain 83, 129, 234, 463, and 1015 ROIs respectively. The number of the fibres (NOF) connecting each pair of ROIs (i, j) and each ROI's surface area (SA) were obtained, and the fiber density (FD) in the connection was obtained by dividing NOF between ROIs (i, j) by the average SA of regions i and j [26]. Finally, the brain networks were constructed using the fiber density of tracts connecting between pairs of ROIs. An example of a subject's structural network at different scales depicted using heatmaps generated from adjacency matrices can be found in Figure 1.

To study the changes in graph theoretical across diagnostic populations, the 173 subjects were organized into three groups. The Healthy Control (HC) group consisted of 76 subjects, including healthy control without symptoms and significant memory concern subjects who were self-perceived to have cognitive decline without objective cognitive impairment [27]. The Mild Cognitive Impairment (MCI) group consisted of 68 subjects, either with early MCI or late MCI. The final AD group consisted of 29 subjects clinically diagnosed with Alzheimer's disease.

B. Network analysis across scales.

We computed 4 network-level graph theoretical measures for comparison, with two global integrative measures and two local segregative measures. The computations were done using the Python implementation of the Brain Connectivity Toolbox (BCT) [28]. For integrative measures, we computed characteristic path length and global efficiency. Characteristic path length is defined as:

$$L = \frac{1}{n}\sum_{i \in N}\frac{\sum_{j \in N, j \neq i} d_{ij}^{w}}{n-1}, \tag{1}$$

which is equivalent to the average of the shortest path lengths in the network [29]. d_{ij}^{w} denotes the distance between nodes (i, j), derived by inverting the edge weight between the two nodes $d_{ij} = 1/w_{ij}$. However, it is noted that in the event that a network is disconnected, path lengths will yield infinities. An alternative approach to measuring integration is thus global efficiency, defined as:

$$E = \frac{1}{n}\sum_{i \in N}\frac{\sum_{j \in N, j \neq i}\left(d_{ij}^{w}\right)^{-1}}{n-1} \tag{2}$$

yielding an inverse relationship with the shortest path length [30]. In the event that a path has infinite length, the global efficiency approaches 0.

For measures of segregation, we computed average clustering coefficient and transitivity. Both of the measures investigate the presence of cliques, or triplets, in the network [29]. Clustering coefficient at the nodal level for the i^{th} node (C_i) is defined as:

$$C_i = \frac{2}{k_i(k_i-1)}\sum_{j,k}\left(w_{ij}w_{jk}w_{ki}\right)^{1/3} \tag{3}$$

where nodes j and k are neighboring nodes and k_i is the degree of node i. To calculate a network average clustering coefficient, the individual nodal clustering coefficients are averaged:

$$C = \frac{1}{n}\sum_{i \in N} C_i\,. \tag{4}$$

An alternative approach to calculate a network-level clustering coefficient is the transitivity, which observes the ratio of the number of closed triplets to the number of total possible triplets [31], [32]. The transitivity is calculated as:

$$T = \frac{\sum_{i \in N} 2\left(w_{ij}w_{jk}w_{ki}\right)^{1/3}}{\sum_{i \in N} k_i(k_i-1)}\,. \tag{5}$$

The 4 network-level graph theoretical measures are computed for each subject at each of the 5 scales of the Lausanne parcellation, yielding a total of 20 measures for each subject.

To compare group differences, Kruskal-Wallis was conducted followed by Dunn posthoc. A false discovery rate (FDR) correction was applied to correct for multiple comparisons. Significance was tested at a 5% level ($P > 0.05$) and the medians of the populations were then compared for directionality analysis.

III. Results

The medians of the computed graph theoretical measures and their relationship with scale are shown in Figure 2. It was observed that the characteristic path length generally increased alongside with parcellation scale, exhibiting the longest median path lengths at Scale 500 (Figure 2C). As global efficiency is related to the inverse characteristic path length, it exhibited the expected trend of decreasing as the parcellation scale was increased (Figure 2D). The average clustering coefficient exhibited a slight increase with parcellation scale (Figure 2A), while transitivity was largely unaffected by the selection of scale (Figure 2B).

Significant group differences were found primarily when comparing the healthy control to the two disease groups (HC vs. MCI, HC vs. AD), with varying degrees of consistency. When observing segregative measures of average clustering coefficient and transitivity, transitivity was the most robust measure, capable of consistently identifying group differences across all scales in the HC vs. MCI and HC vs. AD comparisons. Average clustering coefficient only exhibited significant differences at the lower scale parcellations, showing significant differences in Scales 33 and 60 for the HC vs. MCI comparison ($P = 0.0358$) and in Scales 33, 60, 125, and 250 for the HC vs. AD comparison ($P = 0.0289$) (Table I). The directionality of change in both segregative measures was consistent across scales, where they exhibited a decrease from HC to MCI and an increase from HC to AD (Figure 3A,B). Lastly, no significant differences could be found in the segregative measures when comparing the two disease groups of MCI and AD.

For the two integrative measures of characteristic path length and global efficiency, we found that global efficiency was able to consistently identify group differences between HC and MCI, while characteristic path length was less robust and could only identify group differences between HC and MCI in Scale 33 ($P = 0.0132$), Scale 125 ($P = 0.0289$), and Scale 250 ($P = 0.0203$). Characteristic path length showed a consistent decrease when comparing HC vs. MCI and global efficiency showed a consistent increase in the comparison (Figure 3C,D). In the HC vs. AD comparison, neither of the measures were robust to the change in scale. Characteristic path length only exhibited HC to AD group differences at Scale 250 ($P = 0.0083$), while global efficiency exhibited group differences at Scales 33 ($P = 0.0494$), 250 ($P = 0.0494$), and 500 ($P = 0.0312$) (Table I). Similar to the segregative measures, no significant differences were observed in the integrative measures when comparing between the two diseased groups.

IV. Discussion

The consistency of graph theoretical measures across different methods of graph creation has been a long-standing problem in network neuroscience, whereby changes to parcellation scheme and the number of nodes have an impact on the magnitude of the measures

observed. In prior studies in the field, it was noted that characteristic path length and global efficiency are highly sensitive to the number of nodes [8], [12], while average clustering coefficient and transitivity are less affected by the choice of parcellation [8], [13]. We observe similar relationships between scale and graph theoretical measures in our study, with the integrative measures of characteristic path length and global efficiency being more sensitive to parcellation scale compared transitivity, which exhibited more stability across scales (Figure 2).

A. Significance when comparing disease groups

The effects of scale on graph theoretical measures become more apparent when observing between-groups differences in the measures. It has been posited that differences in graph creation methods are a source of inconsistency in the significance and direction of change in relation to disease state [6]. A previous finding in white matter networks note that both segregative and integrative measures to be inconsistent in identifying group differences when compared across parcellation schemes [15]. Corroborating prior studies, we observed that the integrative measures of characteristic path length and global efficiency were highly sensitive to the choice of parcellation scale, with characteristic path length only finding significance for the HC vs. AD comparison in Scale 250 and global efficiency only finding significance for the HC vs. AD comparison in Scales 33, 250, and 500. In the previous study using fractional anisotropy networks, it is noted that average clustering coefficient in particular struggled to identify group differences at a network level [15]. The weaknesses of average clustering coefficient identified in previous studies thus align with our present findings where average clustering coefficient was unable to distinguish between MCI and AD group networks in any parcellation scale and was unable to distinguish between HC and MCI groups in the higher scales of 125, 250, and 500. Average clustering coefficient's sensitivity to scale and previously identified sensitivty to parcellation scheme may offer an explanation regarding previous studies' struggles to find significance in the measure [6].

The second segregative measure that we investigated, transitivity, showed the greatest robustness against scale, as group differences were identified for HC vs. MCI and HC vs. AD across all parcellation scales. The robustness of transitivity to the selection of scale corroborates previous findings in AD cortical thickness networks, where transitivity was noted to have the greatest stability when altering the number of nodes and parcellation schemes used to create structural networks [13], [14]. As such, we conclude that the segregative measure of transitivity offers the greatest robustness to parcellation-related choices and may offer a more consistent depiction of topological disruption when comparing between healthy and disease-state brain networks.

B. Direction of change with respect to increasing disease severity

In terms of directionality, we found that segregative measures generally increased with disease severity when comparing between HC and AD. These findings align with that of prior studies indicating that the structural connectome eventually becomes more segregated as AD progresses, leading to disrupted connectivity and supporting the hypothesis that AD is a disconnection syndrome [2], [13]–[15], [33], [34]. However, the comparison between HC and MCI depicts the opposite trend in segregative measures, indicating

that early stages of the disease may exhibit an initial decrease in segregation before increasing as the disease worsens. These findings in relation to MCI in clustering coefficient corroborate those of certain studies in MCI structural networks that weighted networks with streamline counts [35], [36], while running against trends found in structural networks using fractional anisotropy [15]. We also found that integrative measures pointed towards increased integration in MCI while being largely insignificant when comparing to AD groups, with decreased characteristic path length and increased global efficiency, again running counter to findings using other weighting methods [15], [35]–[37]. As such, we conclude that there are additional factors that influence the observed directionality of graph theoretical measures that may warrant further study.

V. Conclusion

From this study, we conclude that the selection of parcellation scale has an impact on the observed graph theoretical measures of fiber density networks and their ability to distinguish between diagnostic groups in the ADNI cohort. Most notably, average clustering coefficent, characteristic path length, and global efficiency largely do not maintain significance when the parcellation scale is varied, while transitivity is more robust to the change in scale. The study has thus provided further evidence that these measurements are highly sensitive to brain network creation methods and future study must be conducted to determine more robust measures for quantifying topological disruptions in the context of disease.

Acknowledgment

This work was supported in part by the National Institutes of Health grants T32 AG076411, RF1 AG068191 and U01 AG068057, and the National Science Foundation grant IIS 1837964. Data used in this study were obtained from the Alzheimer's Disease Neuroimaging Initiative database (adni.loni.usc.edu), which was funded by NIH U01 AG024904.

References

[1]. Alzheimer's Association, "2022 Alzheimer's disease facts and figures," Alzheimer's Dementia, vol. 18, no. 4, pp. 700–789, 2022.

[2]. Delbeuck X, Van der Linde M, and Collette F, "Alzheimer's disease as a disconnection syndrome?" Neuropsychology Review, vol. 13, no. 2, pp. 79–92, 2003. [PubMed: 12887040]

[3]. Bassett DS and Sporns O, "Network neuroscience," Nature Neuroscience, vol. 20, no. 3, p. 353–364, 2017. [PubMed: 28230844]

[4]. delEtoile J and Adeli H, "Graph theory and brain connectivity in alzheimer's disease," The Neuroscientist, vol. 23, no. 6, p. 616–626, 2017. [PubMed: 28406055]

[5]. Yu M, Sporns O, and Saykin AJ, "The human connectome in alzheimer disease — relationship to biomarkers and genetics," Nature Reviews Neurology, vol. 17, no. 9, p. 545–563, 2021. [PubMed: 34285392]

[6]. Tijms BM, Wink AM, Haan WD, Flier WMVD, Stam CJ, Scheltens P, and Barkhof F, "Alzheimers disease: connecting findings from graph theoretical studies of brain networks," Neurobiology of Aging, vol. 34, no. 8, p. 2023–2036, 2013. [PubMed: 23541878]

[7]. Svaldi DO, Goñi J, Abbas K, Amico E, Clark DG, Muralidharan C, Dzemidzic M, West JD, Risacher SL, Saykin AJ, and et al. , "Optimizing differential identifiability improves connectome predictive modeling of cognitive deficits from functional connectivity in alzheimer's disease," Human Brain Mapping, vol. 42, no. 11, p. 3500–3516, 2021. [PubMed: 33949732]

[8]. Zalesky A, Fornito A, Harding IH, Cocchi L, Yücel M, Pantelis C, and Bullmore ET, "Whole-brain anatomical networks: Does the choice of nodes matter?" NeuroImage, vol. 50, no. 3, p. 970–983, 2010. [PubMed: 20035887]

[9]. Wang J, Wang L, Zang Y, Yang H, Tang H, Gong Q, Chen Z, Zhu C, and He Y, "Parcellation-dependent small-world brain functional networks: A resting-state fmri study," Human Brain Mapping, vol. 30, no. 5, p. 1511–1523, 2009. [PubMed: 18649353]

[10]. Drakesmith M, Caeyenberghs K, Dutt A, Lewis GH, David AS, and Jones DK, "Overcoming the effects of false positives and threshold bias in graph theoretical analyses of neuroimaging data," NeuroImage, vol. 118, p. 313–333, 2015. [PubMed: 25982515]

[11]. Buchanan CR, Bastin ME, Ritchie SJ, Liewald DC, Madole JW, Tucker-Drob EM, Deary IJ, and Cox SR, "The effect of network thresholding and weighting on structural brain networks in the uk biobank," NeuroImage, vol. 211, p. 116443, 2020.

[12]. Wijk BCMV, Stam CJ, and Daffertshofer A, "Comparing brain networks of different size and connectivity density using graph theory," PLoS ONE, vol. 5, no. 10, 2010.

[13]. Mårtensson G, Pereira JB, Mecocci P, Vellas B, Tsolaki M, Kłoszewska I, Soininen H, Lovestone S, Simmons A, Volpe G, and et al. , "Stability of graph theoretical measures in structural brain networks in alzheimer's disease," Scientific Reports, vol. 8, no. 1, 2018.

[14]. Phillips DJ, McGlaughlin A, Ruth D, Jager LR, and Soldan A, "Graph theoretic analysis of structural connectivity across the spectrum of alzheimer's disease: The importance of graph creation methods," NeuroImage: Clinical, vol. 7, p. 377–390, 2015. [PubMed: 25984446]

[15]. Wu Z, Xu D, Potter T, and Zhang Y, "Effects of brain parcellation on the characterization of topological deterioration in alzheimers disease," Frontiers in Aging Neuroscience, vol. 11, 2019.

[16]. Yu M, Sporns O, and Saykin AJ, "The human connectome in alzheimer disease - relationship to biomarkers and genetics," Nat Rev Neurol, vol. 17, no. 9, pp. 545–563, 2021. [PubMed: 34285392]

[17]. Yaakub SN, Heckemann RA, Keller SS, McGinnity CJ, Weber B, and Hammers A, "On brain atlas choice and automatic segmentation methods: A comparison of maper amp; freesurfer using three atlas databases," Scientific Reports, vol. 10, no. 1, 2020.

[18]. Weiner MW, Veitch DP, Aisen PS, Beckett LA, Cairns NJ, Green RC, Harvey D, Jack CR, Jagust W, Liu E, Morris JC, Petersen RC, Saykin AJ, Schmidt ME, Shaw L, Shen L, Siuciak JA, Soares H, Toga AW, Trojanowski JQ, and Alzheimer's Disease Neuroimaging I, "The alzheimer's disease neuroimaging initiative: a review of papers published since its inception," Alzheimers Dement, vol. 9, no. 5, pp. e111–94, 2013. [PubMed: 23932184]

[19]. Weiner MW, Aisen PS, Jack CR, Jagust WJ, Trojanowski JQ, Shaw L, Saykin AJ, Morris JC, Cairns N, and Beckett LA, "The alzheimer's disease neuroimaging initiative: Progress report and future plans," Alzheimer's amp; Dementia, vol. 6, no. 3, p. 202, 2010.

[20]. Saykin AJ, Shen L, Yao X, Kim S, Nho K, Risacher SL, Ramanan VK, Foroud TM, Faber KM, and Sarwar N, "Genetic studies of quantitative mci and ad phenotypes in adni: Progress, opportunities, and plans," Alzheimer's amp; Dementia, vol. 11, no. 7, p. 792–814, 2015.

[21]. Li H, Fang S, Contreras JA, West JD, Risacher SL, Wang Y, Sporns O, Saykin AJ, Goni J, Shen L, and Alzheimer's Disease Neuroimaging I, "Brain explorer for connectomic analysis," Brain Inform, vol. 4, no. 4, pp. 253–269, 2017. [PubMed: 28836134]

[22]. Manjón JV, Coupé P, Concha L, Buades A, Collins DL, and Robles M, "Diffusion weighted image denoising using overcomplete local pca," PLoS ONE, vol. 8, no. 9, 2013.

[23]. Moore C and Sciacca F, "Fiber assignment by continuous tracking algorithm (fact)," Radiopaedia.org, 2019.

[24]. Jenkinson M, Beckmann CF, Behrens TE, Woolrich MW, and Smith SM, "Fsl," NeuroImage, vol. 62, no. 2, p. 782–790, 2012. [PubMed: 21979382]

[25]. Cammoun L, Gigandet X, Meskaldji D, Thiran JP, Sporns O, Do KQ, Maeder P, Meuli R, and Hagmann P, "Mapping the human connectome at multiple scales with diffusion spectrum mri," Journal of Neuroscience Methods, vol. 203, no. 2, p. 386–397, 2012. [PubMed: 22001222]

[26]. Yan J, Raja VV, Huang Z, Amico E, Nho K, Fang S, Sporns O, Wu YC, Saykin A, Goñi J, and Shen L, "Brain-wide structural connectivity alterations under the control of alzheimer risk

genes," International Journal of Computational Biology and Drug Design, vol. 13, no. 1, p. 58, 2020. [PubMed: 32095160]

[27]. Zhang J, Zhou W, Cassidy RM, Su H, Su Y, and Zhang X, "Risk factors for amyloid positivity in older people reporting significant memory concern," Comprehensive Psychiatry, vol. 80, p. 126–131, 2018. [PubMed: 29091778]

[28]. Rubinov M and Sporns O, "Complex network measures of brain connectivity: Uses and interpretations," NeuroImage, vol. 52, no. 3, p. 1059–1069, 2010. [PubMed: 19819337]

[29]. Watts DJ and Strogatz SH, "Collective dynamics of 'small-world'networks," nature, vol. 393, no. 6684, pp. 440–442, 1998. [PubMed: 9623998]

[30]. Latora V and Marchiori M, "Efficient behavior of small-world networks," Physical review letters, vol. 87, no. 19, p. 198701, 2001. [PubMed: 11690461]

[31]. Wasserman S and Faust K, "Social network analysis: Methods and applications," Cambridge University Press, p. 435, 1994.

[32]. Opsahl T and Panzarasa P, "Clustering in weighted networks," Social Networks, vol. 31, no. 2, p. 155–163, 2009.

[33]. He Y, Chen Z, and Evans A, "Structural insights into aberrant topological patterns of large-scale cortical networks in alzheimer's disease," Journal of Neuroscience, vol. 28, no. 18, p. 4756–4766, 2008. [PubMed: 18448652]

[34]. Lo C-Y, Wang P-N, Chou K-H, Wang J, He Y, and Lin C-P, "Diffusion tensor tractography reveals abnormal topological organization in structural cortical networks in alzheimer's disease," Journal of Neuroscience, vol. 30, no. 50, p. 16876–16885, 2010. [PubMed: 21159959]

[35]. Berlot R, Metzler-Baddeley C, Ikram MA, Jones DK, and O'Sullivan MJ, "Global efficiency of structural networks mediates cognitive control in mild cognitive impairment," Frontiers in Aging Neuroscience, vol. 08, 2016.

[36]. Bergamino M, Walsh RR, and Stokes AM, "Analysis of brain structural connectivity networks and white matter integrity in patients with mild cognitive impairment," Alzheimer's amp; Dementia, vol. 17, no. S5, 2021.

[37]. Reijmer YD, Leemans A, Caeyenberghs K, Heringa SM, Koek HL, Biessels GJ, Group UVCIS et al. , "Disruption of cerebral networks and cognitive impairment in alzheimer disease," Neurology, vol. 80, no. 15, pp. 1370–1377, 2013. [PubMed: 23486876]

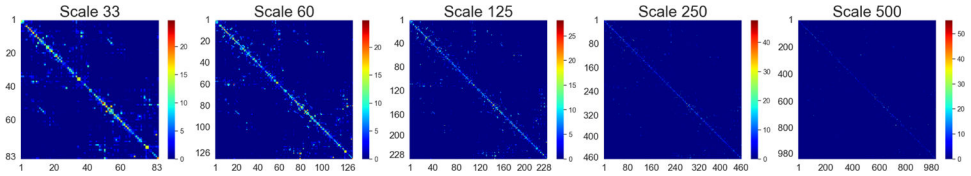

Fig. 1.

An example of the structural connectome derived using fiber density is shown at 5 different scales for a healthy control subject (scales 33, 60, 125, 250, and 500). The heatmaps are generated from the adjacency matrices of each structural network, with the axes being the ROIs ordered by their index number in the parcellation scheme. It can be seen that as the scale is increased, the connections become significantly more sparse.

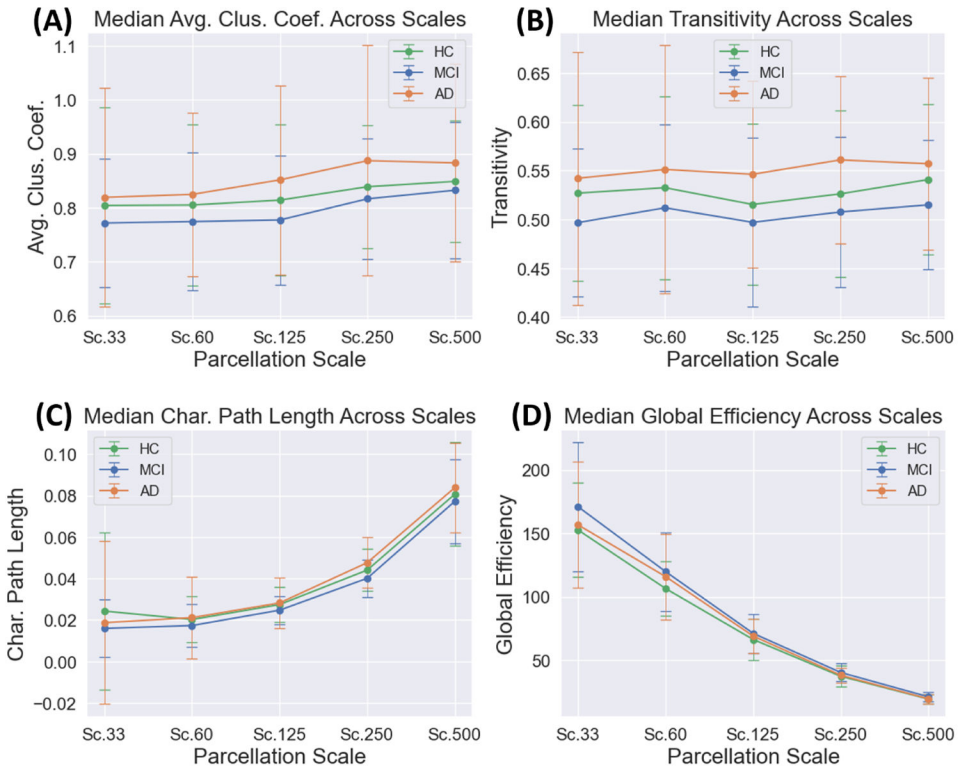

Fig. 2.

The median values of the 4 graph theoretical measures are plotted with respect to parcellation scale. We can observe that the two segregative measures of average clustering coefficient (A) and transitivity (B) are less sensitive to scale than the integrative measures of characteristic path length (C) and global efficiency (D).

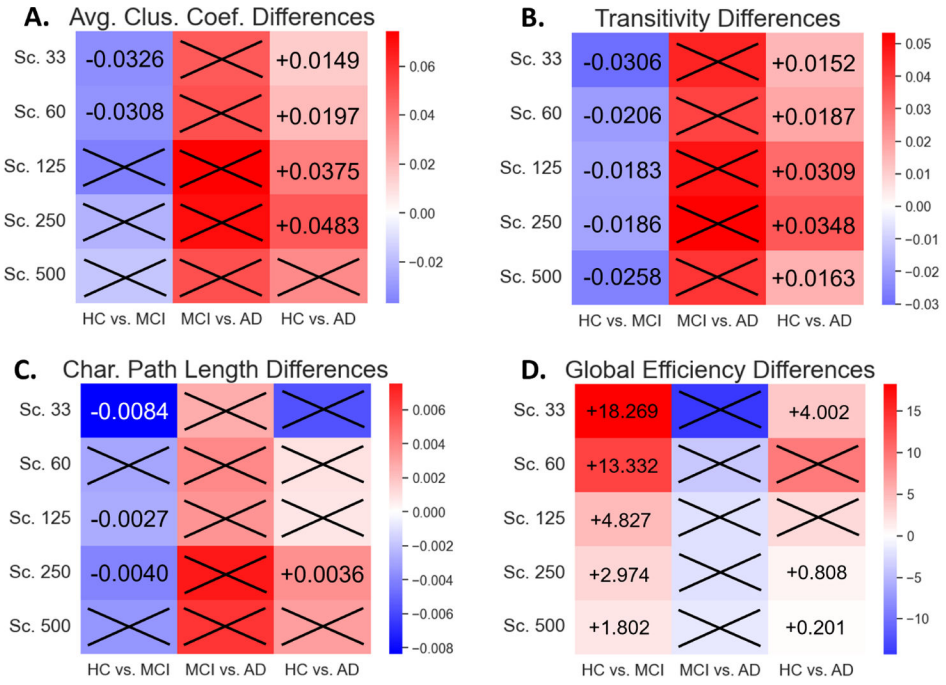

Fig. 3.

Heatmaps were constructed to depict the directionality of change in the network measurements with respect to increasing disease severity. The first column in each subplot is the difference when progressing from HC to MCI, the second is from MCI to AD, and the third is from HC to AD. Red coloration indicates that the measure increases as disease severity increases, while blue coloration indicates that the measure decreases as disease severity increases. Results are shown for average clustering coefficient (A), transitivity (B), characteristic path length (C), and global efficiency (D). Numerical labels indicate the difference in medians between the two groups with respect to increasing disease severity.

TABLE I

Posthoc Dunn P-Values

	Avg. Clus. Coef.			Transitivity		
Scale	**HC vs. MCI**	**MCI vs. AD**	**HC vs. AD**	**HC vs. MCI**	**MCI vs. AD**	**HC vs. AD**
33	**0.0203**	0.7962	**0.0358**	**0.0289**	0.6296	**0.0358**
60	**0.0494**	0.4579	**0.0289**	**0.0289**	0.4140	**0.0184**
125	0.1230	0.2201	**0.0210**	**0.0494**	0.2689	**0.0151**
250	0.0710	0.2969	**0.0210**	**0.0290**	0.2128	**0.0083**
500	0.3107	0.6677	0.2378	**0.0229**	0.2689	**0.0083**
	Char. Path Length			**Glob. Efficiency**		
Scale	**HC vs. MCI**	**MCI vs. AD**	**HC vs. AD**	**HC vs. MCI**	**MCI vs. AD**	**HC vs. AD**
33	**0.0132**	0.5440	0.1970	**0.0083**	0.8217	**0.0494**
60	0.0752	0.7438	0.0958	**0.0105**	0.4569	0.2006
125	**0.0289**	0.8259	0.0563	**0.0132**	0.6677	0.1230
250	**0.0203**	0.2712	**0.0083**	**0.0083**	0.7962	**0.0494**
500	0.3107	0.5835	0.1970	**0.0083**	0.9889	**0.0312**

Significant *P*-values are highlighted in bold, tested at a 5% level, FDR-corrected.

Proceedings (IEEE Int Conf Bioinformatics Biomed). Author manuscript; available in PMC 2024 January 02.